IEEE Access
Multidisciplinary | Rapid Review | Open Access Journal

Received May 23, 2017, accepted September 11, 2017, date of current version October 25, 2017.

Digital Object Identifier 10.1109/ACCESS.2017.2752198

Effective Interference Nulling Virtual MIMO Broadcasting Transceiver for Multiple Relaying

BEOM KWON AND SANGHOON LEE, (Senior Member, IEEE)
Department of Electrical and Electronic Engineering, Yonsei University, Seoul 120-749, South Korea

Corresponding author: Sanghoon Lee (slee@yonsei.ac.kr)

This work was supported by the Basic Science Research Program through the National Research Foundation of Korea (NRF), Ministry of Education, under Grant NRF-2013R1A1A2A10011764.

ABSTRACT In multi-hop relay networks, the improving end-to-end sum rate is a challenging issue. Although a new cooperative beamforming called virtual multiple-input multiple-output (MIMO) has been introduced as a possible solution, conventional virtual MIMO systems have severe signaling overhead among master and source nodes when the number of hops increases. To resolve this problem, a broadcast virtual MIMO system and a virtual MIMO broadcasting transceiver (VMBT) have been proposed to reduce the computational complexity and improve the end-to-end sum rate. However, the application of such methods is limited to environments wherein interference from other links and networks is not considered. Thus, it is difficult to apply them to practical multi-hop relay networks. In this paper, we propose a generalized version of the VMBT in which intra- and inter-network interferences are simultaneously caused by multiple transmission of clusters in the same network and each network's usage of the same frequency band, respectively. To achieve this goal, we propose an effective interference nulling VMBT scheme. Simulation results show that the proposed scheme has efficient performance in terms of average end-to-end sum rate compared with conventional schemes.

INDEX TERMS Effective interference nulling, multiple transmission, single frequency network, virtual MIMO broadcasting transceiver.

I. INTRODUCTION

Increasing the end-to-end sum rate in wireless ad-hoc networks is required in many applications, such as smart cities [1], smart grid [2], Internet of Things (IoT) [3], and alert systems for natural disasters [4]. In wireless ad-hoc networks, sensor nodes should communicate with each other at high link capacity for a given power limitation. In addition, in recent years, the demand for multimedia services over wireless ad-hoc networks has significantly increased, increasing the need for a technique for achieving high link capacity [5], [6]. Toward this goal, cooperative beamforming (BF) using a multiple-input multiple-output (MIMO) technique has been considered. However, cooperative BF has been primarily investigated for cellular networks [7]–[10] and cellular-based relay networks [11]–[13]. In [7]–[13], the role of network components such as base and relay stations is predetermined, and each base (relay) station knows the topology of network including the location information of each other. In addition, it is assumed that transmit data and channel state information for cooperative BF among base stations and relay stations are exchanged via wired backhaul. On the other hand, in general wireless ad-hoc networks, the role of each node is changed dynamically based on detection of event and residual energy among nodes. Moreover, there is no network infrastructure such as wired backhaul. Therefore, each node needs to update the identity and location information of its adjacent nodes for cooperative BF. In contrast to cellular and cellular-based relay networks, practically, it is inefficient to share the channel information among nodes due to uncertainty of role and lack of resource.

To overcome this difficulty, a new cooperative BF technique called virtual MIMO has been introduced by the authors [14], [15]. In conventional virtual MIMO systems, each cluster is composed of adjacent nodes equipped with a single antenna, and the cluster performs like a multiple-antenna node. To transmit a signal cooperatively to a

2169-3536 © 2017 IEEE. Translations and content mining are permitted for academic research only.
Personal use is also permitted, but republication/redistribution requires IEEE permission.
See http://www.ieee.org/publications_standards/publications/rights/index.html for more information.

neighboring cluster, the source node must first transmit the signal to adjacent nodes in the same cluster. Moreover, each cluster must have a master node that gathers the received signal from adjacent nodes in the same cluster, decodes the symbols, and retransmits them to the adjacent nodes. In addition, the master node must collect the intra-cluster channel information to construct the BF vector required to transmit such channel information to the next cluster. Therefore, in conventional virtual MIMO systems, additional time redundancy is required to gather, decode, and retransmit data symbols, and signaling overhead associated with intra-clustering channel information is also required. These factors decrease the performance of conventional virtual MIMO-based wireless ad-hoc networks. In addition, the complexity of such wireless ad-hoc networks exponentially increases with the number of hops because of the high signaling overhead and low time efficiency.

This problem has been one of the most challenging issues in virtual MIMO-based wireless ad-hoc networks using multiple-antenna nodes [16]–[18]. Although virtual MIMO relay systems using multiple-antenna nodes have been studied [19]–[21], the issue has not been resolved.

To address signaling overhead, we proposed a broadcast virtual MIMO system (BVMS) to reduce the complexity of virtual MIMO relay systems [22]. Since the BVMS does not require a master node, it is not necessary to gather the received signal, decode symbols, or collect intra-cluster channel information to construct a BF vector at the master node. Thus, the BVMS effectively reduces the complexity and time redundancy compared with conventional virtual MIMO systems. In addition, to improve the end-to-end sum rate of the BVMS, the max-min (M^2) BF technique has been proposed [22]. However, the M^2 BF technique is designed for a limited environment where each node is equipped with a single antenna. Therefore, if each node is equipped with multiple-antennas in the BVMS, applying this technique to the BVMS is difficult. To overcome this limitation, we have developed a framework to design a virtual MIMO broadcasting transceiver (VBMT) for the BVMS [23]. A VMBT based on the channel ellipse property (VMBT-CEP) and the iterative algorithm of the VMBT (IA-VMBT) have been proposed to construct a receive weight vector, which was not included in [22].

However, M^2 BF [22], VMBT-CEP, and IA-VMBT [23] can be applied to a limited environment assuming that each network is a multiple frequency network (MFN), such that inter-network interference does not occur. In addition, for multi-hop relay transmission, it is also assumed that only one cluster transmits the signal to the next cluster while the other clusters wait their turn (single transmission; ST); thus, intra-network interference does not occur. In other words, inter- and intra-network interferences are not considered in [22] and [23].

To adapt the BVMS to a practical wireless ad-hoc network, it is necessary to address the performance degradation problem caused by intra- and inter-network interferences. In order to reduce the interferences, zero-forcing beamforming (ZF-BF) techniques have been researched by using the full channel information [24]–[26]. When the channel vectors of the selected nodes in the receive cluster are orthogonal with each other, a higher sum rate throughput can be obtained. In general, as the number of nodes in the receive cluster increases, the sum rate performance becomes better. ZF-BF techniques utilize the multi-node diversity gain to achieve high sum rate throughput. However, if the number of nodes in the receive cluster is not enough to obtain the diversity gain, poor performance could be observed. In general, the performance of ZF-BF techniques decreases as the number of nodes also decreases. After all, it is difficult to select the nodes whose channel vectors are orthogonal to each other. In general virtual MIMO systems including the BVMS, each cluster has fewer nodes, which makes it difficult to achieve the multi-node diversity gain with ZF-BF techniques. Therefore, it is necessary to develop a suitable interference handling scheme for the BVMS in which multi-node diversity cannot be fully utilized. Therefore, in this study, we propose an effective interference nulling VMBT (EIN-VMBT) scheme for the BVMS when such interferences occur. In addition, to obtain a general solution, it is assumed that each node is equipped with multiple antennas.

The main contributions of this study are as follows. (1) Based on previous studies [22], [23], we develop a complete BVMS for a practical wireless ad-hoc network that is generalized with multiple antennas and intra- and inter-network interferences' parameters to overcome performance degradation due to interference. (2) In a generalized interference environment where intra- and inter-network interferences occur, we propose EIN-VMBT. EIN-VMBT eliminates interference to achieve a high end-to-end sum rate for the BVMS. When intra- and inter-network interferences occur, the proposed EIN-VMBT improves the average end-to-end sum rate compared with conventional schemes. (3) To construct suboptimal transmit and receive weight vectors of each cluster, we propose an iterative algorithm that converges within less than five iterations on average. (4) In addition, to maximize the multi-hop link capacity, we propose a criterion for selection of ST and multiple transmission (MT), and a transmit power control scheme.

In Table 1, the conventional and proposed schemes are summarized and compared in terms of master node, transmit weight vector, receive weight vector, frequency band, multi-hop transmission, and interference. In singular value decomposition (SVD)-based BF, the master node in each cluster must gather the received signal from adjacent nodes in the same cluster [16]–[18]. In contrast, in BVMS-based schemes, such as M^2 BF, VMBS-CEP, IA-VMBS, and EIN-VMBS, the master node does not need to gather the received signal from adjacent nodes in the same cluster.

In SVD BF, the transmit (receive) weight vector is constructed using the first right (left) singular vector of the channel matrix, which corresponds to the largest singular value. In M^2 BF, the transmit weight vector is designed to maximize

TABLE 1. Comparison of conventional and proposed schemes.

Scheme		Master node	Transmit weight vector	Receive weight vector	Frequency band	Multi-hop transmission	Interference
Conventional schemes	SVD BF [16-18]	O	First right singular vector of the channel matrix	First left singular vector of the channel matrix	MFN	Single transmission	X
	M^2 BF [22]	X	Construct transmit weight vector using GO M^2 BF	X	MFN	Single transmission	X
	VMBT-CEP [23]	X	Construct transmit weight vector using GO M^2 BF w.r.t. receive weight vector	Construct receive weight vector using CEP	MFN	Single transmission	X
	IA-VMBT [23]	X		Construct receive weight vector using IA	MFN	Single transmission	X
Proposed scheme	EIN-VMBT	X		Construct receive weight vector using EIN	SFN, MFN	Single and multiple transmissions	Intra- and inter-network interferences

the minimum capacity in the same cluster and is constructed using the global optimal (GO) M^2 BF. In addition, constructing the receive weight vector is not necessary because M^2 BF is designed for an environment with single-antenna nodes. VMBT-CEP, IA-VMBT, and EIN-VMBT construct the transmit weight vector with regard to the receive weight vector using GO M^2 BF. In VMBT-CEP and IA-VMBT, the receive weight vector is constructed to maximize the minimum link capacity of the channels. However, the receive weight vector in EIN-VMBT is constructed to eliminate intra- and inter-network interferences.

As shown in Table 1, the conventional schemes (SVD BF, M^2 BF, VMBT-CEP, and IA-VMBT) do not consider intra- and inter-network interferences because these schemes are designed for ideal interference-free environments based on ST over MFN. On the other hand, EIN-VMBT is designed for an environment where more than one cluster transmits signals simultaneously and all the networks share the same frequency band; consequently, intra- and inter-network interferences do occur.

The remainder of this paper is organized as follows. In Section II, the motivation for this study is described through a comparison of the relay method for a conventional virtual MIMO system (CVMS), BVMS-ST, and BVMS-MT. In Section III, the system model for the BVMS-MT over a single frequency network (SFN) where each node has multiple antennas is described. In Section IV, the proposed EIN-VMBT, which maximizes link capacity and effectively eliminates intra- and inter-network interferences, is described. Simulation results are provided in Section V, and conclusions are presented in Section VI.

II. MOTIVATION

Fig. 1 shows how a signal is delivered from the source to a destination node according to each scheme. In CVMS, the master node in each cluster gathers the received signals from adjacent nodes, decodes the symbol, and retransmits it to adjacent nodes. Then, all nodes including the master node in the cluster decode the symbol and transmit it to the next cluster. On the other hand, in BVMS, each adjacent node decodes the symbol individually and broadcasts it to nodes in the next cluster at the next time slot. In CVMS and BVMS-ST, this procedure is consecutively performed until the signal is sent to the destination node. In addition, since only one cluster transmits the signal to the next cluster in conventional schemes based on CVMS and BVMS-ST, as shown in Table 1, it is not necessary to consider interference caused by other clusters.

However, in multi-hop relay networks, it may be possible to obtain higher link capacity when multiple clusters simultaneously transmit signals even if intra-network interference occurs. For this reason, BVMS-MT is considered. To achieve high link capacity, the source node in BVMS-MT transmits a new signal even though the other cluster still transmits the previous signal, as shown in Fig. 1. Fig. 2 provides an example of BVMS-MT in which the two clusters simultaneously transmit signals to the next clusters. As shown in Fig. 2, intra-network interference occurs and it may cause performance degradation at nodes in the receive clusters l and l'. However, in this study, it is assumed that the receive cluster l' undergoes relatively low interference from the transmit cluster $l-1$, as shown in Fig. 2. Thus, it is assumed that interference is negligible and the transmit cluster $l'-1$ can construct its transmit weight vector using conventional IA-VMBT without considering interference from the transmit cluster $l-1$.

To alleviate performance degradation at cluster l caused by intra-network interference and improve link capacity between clusters $l-1$ and l, we focus on how the transmit cluster $l-1$ and the receive cluster l construct BF vectors. In particular, the proposed EIN-VMBT enables the transmit cluster $l-1$ to construct its transmit weight vector without the receive weight vector information from the receive cluster l. In addition, the receive cluster l constructs its receive weight vector to eliminate intra-network interference from the next transmit cluster $l'-1$. Details of the EIN-VMBT procedure for MT are presented in Section IV-A.

According to the volume of interference, which depends on the transmit power of each transmit cluster, it is possible that the link capacity achieved by ST will increase more than the link capacity achieved by MT. In addition, it is possible

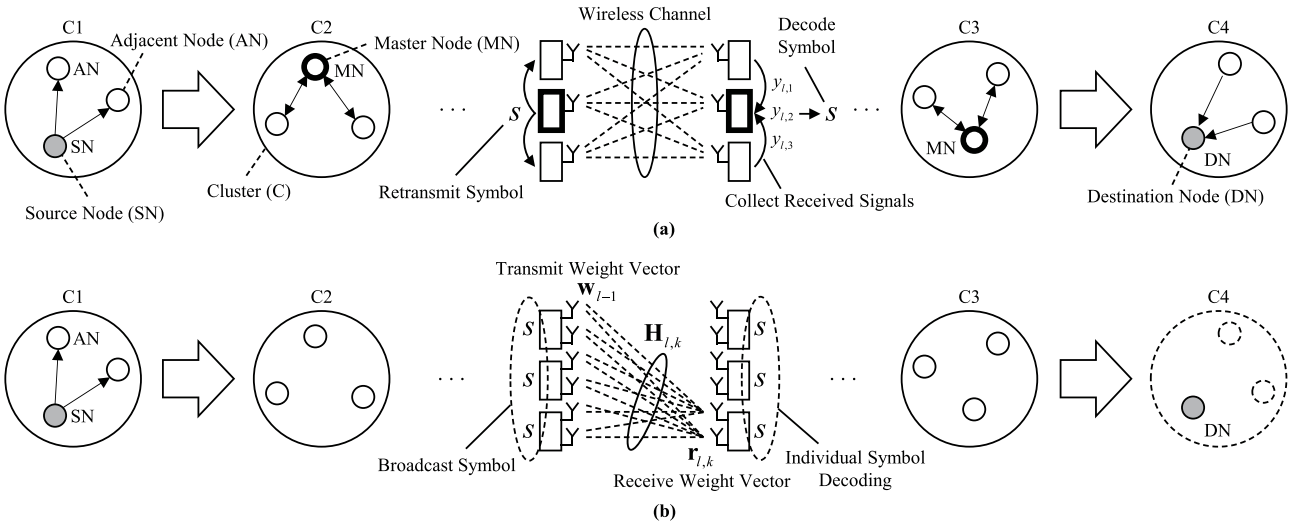

Time Slot / Scheme	1	2	3	4	5	6	7	8	9
CVMS	SN→ANs	ANs→ANs	ANs→MN	MN→ANs	ANs→ANs	ANs→MN	MN→ANs	ANs→ANs	ANs→DN
	C1	C1→C2	C2		C2→C3	C3		C3→C4	C4
BVMS-ST	SN→ANs	ANs→ANs	ANs→ANs	ANs→DN	SN→ANs	ANs→ANs	ANs→ANs	ANs→DN	· · ·
	C1	C1→C2	C2→C3	C3→C4	C1	C1→C2	C2→C3	C3→C4	· · ·
BVMS-MT	SN→ANs	ANs→ANs	ANs→ANs	ANs→DN	SN→ANs	ANs→ANs	ANs→ANs	ANs→DN	· · ·
	C1	C1→C2	C2→C3	C3→C4	C1	C1→C2	C2→C3	C3→C4	· · ·
			SN→RNs	ANs→ANs	ANs→ANs	ANs→DN	SN→ANs	ANs→ANs	· · ·
			C1	C1→C2	C2→C3	C3→C4	C1	C1→C2	· · ·

FIGURE 1. Relay procedure for CVMS and BVMS. (a) CVMS for a node equipped with single antenna. (b) BVMS for a node equipped with multiple antennas.

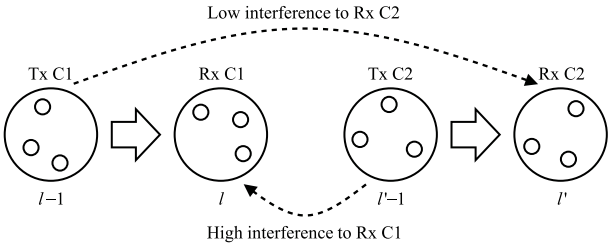

FIGURE 2. Example of BVMS-MT when two clusters transmit signals simultaneously.

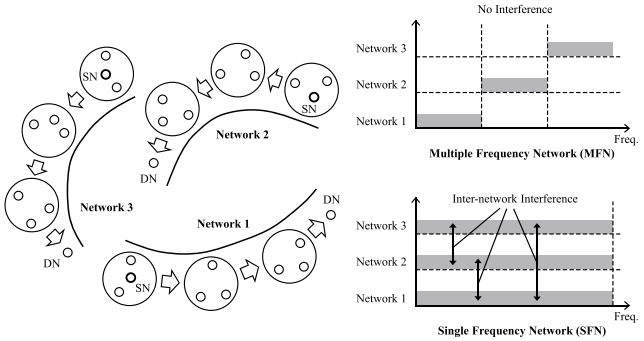

FIGURE 3. Schematic illustration of the BVMS over MFN and SFN.

that the link capacity obtained by MT can be increased by controlling the transmit power of each transmit cluster. Therefore, it is necessary to find a criterion for the selection of ST and MT, and a transmit power control strategy to achieve high link capacity. Toward this goal, multi-hop power control for MT is proposed in Section IV-B. The feasibility of simultaneous transmission and multi-hop power control is measured through algorithm development and performance measurement.

Fig. 3 shows a schematic illustration of the BVMS over MFN and SFN. In SFN, since all networks use the overall frequency bandwidth, the frequency efficiency of SFN can be better than that of MFN. In addition, if interference from other networks is reduced by employing an interference nulling scheme, the overall link capacity of an SFN will be greater. However, since conventional schemes (SVD-BF, M^2 BF, VMBT-CEP, and IA-VMBT) do not consider inter-network interference, using such schemes for an SFN is ineffective. To achieve high overall link capacity and eliminate inter-network interference, we focus on how the transmit cluster $l-1$ and the receive cluster l construct their BF vectors in EIN-VMBT. The procedure of EIN-VMBT over an SFN is detailed in Section IV-C.

III. SYSTEM MODEL

The generalized network architecture is described in this section. In this paper, a wireless mesh network topology is considered and each node autonomously constructs its own cluster with the adjacent nodes. In order to figure out which nodes are the adjacent nodes, some nodes which are selected randomly broadcast an advertisement message to the rest of the nodes. The rest of the nodes measure the signal strength of the advertisement message and report their measurement information to the nodes which broadcasted the advertisement message. Therefore, it is possible for the nodes to know which nodes are the adjacent nodes. Then, each cluster is formed based on the signal strength. When a node detects an event, it becomes a source node. In addition, the cluster which includes the source node becomes a source cluster. A destination node is selected randomly and the cluster which includes the destination node becomes the destination cluster. Then, the other clusters excluding the source and destination clusters become relay clusters.

In this architecture, multiple clusters simultaneously transmit signals, each network uses the same frequency band, and intra- and inter-network interferences simultaneously occur. Let L be the number of clusters, l be the cluster index, $l \in \{1, \cdots, L\}$, T be the number of networks, t be the network index, $t \in \{1, \cdots, T-1\}$, and K_l be the number of nodes in cluster l. It is assumed that each node has M antennas. The receive signal for node k in cluster l can be expressed as

$$\mathbf{y}_{l,k} = \mathbf{H}_{l,k}\mathbf{w}_{l-1}s + \underbrace{\mathbf{H}^{I}_{l,k}\mathbf{w}_{l'-1}s'}_{\substack{\text{intra-network}\\ \text{interference}}} + \underbrace{\sum_{t=1}^{T-1}\sum_{c=1}^{2}\mathbf{H}^{I}_{l,k,t,c}\mathbf{w}_{t,c}s_{t,c}}_{\substack{\text{inter-network}\\ \text{interference}}} + \mathbf{n}_{l,k} \quad (1)$$

where $\mathbf{H}_{l,k}$ is an $M \times K_{l-1}M$-dimensional virtual MIMO channel matrix between the nodes in cluster $l-1$; $\mathbf{w}_{l-1}$ is the $K_{l-1}M \times 1$-dimensional transmit weight vector at cluster $l-1$ ($\|\mathbf{w}_{l-1}\| = 1$) and node k in cluster l; s is the transmit symbol from cluster $l-1$; $\mathbf{H}^{I}_{l,k}$ is the interference channel matrix to node k in cluster l; $\mathbf{w}_{l'-1}$ is the transmit weight vector of cluster l'; s' is the symbol from the other cluster $l'-1$; c is transmit cluster index; $\mathbf{H}^{I}_{l,k,t,c}$ is the interference channel matrix between node k in cluster l and transmit cluster c from network t; $\mathbf{w}_{t,c}$ and $s_{t,c}$ are the transmit weight vector and symbol in transmit cluster c from network t, respectively; and $\mathbf{n}_{l,k}$ is an $M \times 1$-dimensional noise vector at node k in cluster l. Here, it is assumed that all elements of $\mathbf{H}_{l,k}$ are independent with each other and have the same complex zero-mean Gaussian distribution. The element of the i^{th} row and j^{th} column of $\mathbf{H}_{l,k}$ can be expressed as

$$[\mathbf{H}_{l,k}]_{i,j} = \frac{1}{\sqrt{(d_{i,j})^{\eta}}}z_{i,j} \quad (2)$$

where $d_{i,j}$ is the distance between the nodes in cluster $l-1$ and node k in cluster l, η is the path loss exponent, and $z_{i,j}$ is a zero-mean unit-variance complex Gaussian random variable.

In general, it is difficult to simultaneously eliminate intra- and inter-network interferences. Therefore, in this study, eliminating the dominant interference between intra- and inter-network interferences is considered a possible solution. Thus, it is necessary for a transmit cluster to know which interference is more dominant to link capacity. Toward this goal, a time-synchronized network model is applied, as shown in Fig. 4. In the time-synchronized network, each node autonomously constructs its own cluster with the adjacent nodes, and the time slot of a cluster is synchronized with that of other clusters. In addition, a sleep-wake scheduling protocol [27], [28] based on the periodic exchange of information with a neighboring cluster is applied for network configuration.

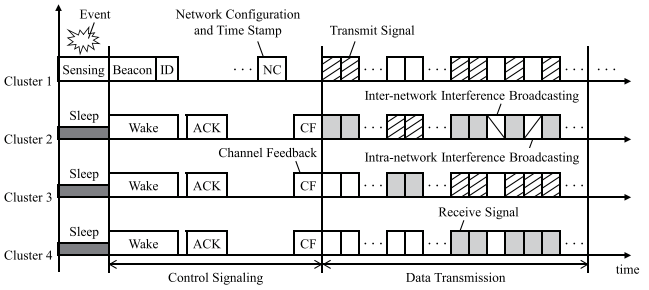

FIGURE 4. Time-synchronized network model for EIN-VMBT.

As shown in Fig 4, if the source cluster (cluster 1) has an event and data to transmit, it sends a beacon signal that includes its cluster ID to find its receive and destination clusters. If a cluster receives the beacon signal over a threshold, it becomes a candidate receive cluster. In addition, the cluster sends an acknowledgement signal to the source cluster that includes its cluster ID. After the source cluster receives the signals from the candidates, it determines the destination cluster and the receive clusters among the candidates. In addition, the source cluster transmits a notification signal that includes time stamp information to measure intra- and inter-network interferences, and the destination and receive clusters transmit their channel information to the source cluster for cooperative BF. This control procedure is performed over the time interval via the control signaling shown in Fig. 4.

After this connection setup is complete, the source cluster transmits data. To measure inter-network interference, transmit clusters in the same network do not transmit any data at the time appointed by the time stamp information transmitted from the source cluster via control signaling. In addition, the receive cluster broadcasts measured the inter-network interference information to its transmit cluster. To measure intra-network interference from the other transmit cluster located in the same network, one transmit cluster does not transmit anything during the transmission of the other transmit cluster at the appointed time. During this time,

the receive cluster measures intra-network interference and broadcasts this information to its transmit cluster. In addition, it is assumed that the measurement of intra- and inter-network interferences is alternatively repeated during data transmission.

Through the above procedure, it is possible for the transmit cluster to receive information about intra- and inter-network interferences and determine which type of interference is more dominant to link capacity. According to the dominant interference, the procedure of constructing transmit and receive weight vectors that eliminate dominant interference and maximize link capacity is described in the next section.

IV. EFFECTIVE INTERFERENCE NULLING VMBT

A. EFFECTIVE INTRA-NETWORK INTERFERENCE NULLING VMBT

For simplification, it is assumed that intra-network interference is dominant to link capacity and that the influence of inter-network interference is comparatively negligible. Then, the receive signal in (1) can be written as follows.

$$\mathbf{y}_{l,k} = \mathbf{H}_{l,k}\mathbf{w}_{l-1}s + \mathbf{H}^{I}_{l,k}\mathbf{w}_{l'-1}s' + \mathbf{n}_{l,k} \tag{3}$$

Since the capacity depends on the minimum capacity among the links, the capacity of cluster l can be written as

$$\min_{k} \log_2 \left(1 + \frac{|\mathbf{r}_{l,k}\mathbf{H}_{l,k}\mathbf{w}_{l-1}|^2}{|\mathbf{r}_{l,k}\mathbf{H}^{I}_{l,k}\mathbf{w}_{l'-1}|^2 + N}\right) \tag{4}$$

where $\mathbf{r}_{l,k}$ is the $1 \times M$-dimensional receive weight vector for node k in cluster l and $N = E[|\mathbf{r}_{l,k}\mathbf{n}_{l,k}|^2]$ is the noise variance.

To eliminate interference and improve the capacity in (4), the receive nodes in receive cluster l construct the receive weight vector. In addition, it is assumed that the transmit cluster $l-1$ in Fig. 2 has $\mathbf{H}^{I}_{l,k}$ and $\mathbf{w}_{l'-1}$ through feedback from the receive nodes and from another transmit cluster $l'-1$, respectively. Therefore, the signaling overhead required to acquire the knowledge of $\mathbf{H}^{I}_{l,k}$ and $\mathbf{w}_{l'-1}$ occurs. The information is transmitted only once to the transmit cluster $l-1$ at the initial stage before performing EIN-VMBT. Through $\mathbf{H}^{I}_{l,k}$ and $\mathbf{w}_{l'-1}$ fed back from each receive node, the transmit cluster $l-1$ knows that each receive node will construct the receive weight vector $\mathbf{r}_{l,k}$ to eliminate the interference $\mathbf{H}^{I}_{l,k}$. Therefore, the transmit cluster $l-1$ constructs its weight vector $\mathbf{w}_{l-1}$ based on interference nulling at the receive cluster l.

Let $\mathbf{b}_M = \mathbf{H}^{I}_{l,k}\mathbf{w}_{l'-1}/\|\mathbf{H}^{I}_{l,k}\mathbf{w}_{l'-1}\|$ and $\mathbf{b}_1, \cdots, \mathbf{b}_M$ be orthonormal to each other ($\mathbf{b}_i^H\mathbf{b}_j = 0, \|\mathbf{b}_i\| = 1, i \neq j$ where the superscript H indicates conjugate transpose). The vectors $\mathbf{b}_1, \cdots, \mathbf{b}_{M-1}$ are the basis of Null($\mathbf{b}_M^T$), where the superscript T indicates transpose. Using $\mathbf{b}_i$, $\mathbf{H}_{l,k}\mathbf{w}_{l-1}$ can be written as

$$\mathbf{H}_{l,k}\mathbf{w}_{l-1} = \sum_{i=1}^{M-1} a_i\mathbf{b}_i + a_M\mathbf{b}_M \tag{5}$$

where a_i is the complex value representing the magnitude and phase of the $\mathbf{b}_i$ component in $\mathbf{H}_{l,k}\mathbf{w}_{l-1}$. The receive weight vector $\mathbf{r}_{l,k}$ comprises $\mathbf{b}_1^H, \cdots, \mathbf{b}_{M-1}^H$ to satisfy the condition $\mathbf{r}_{l,k}\mathbf{H}^{I}_{l,k}\mathbf{w}_{l'-1} = 0$ for interference nulling. To maximize $|\mathbf{r}_{l,k}\mathbf{H}_{l,k}\mathbf{w}_{l-1}|$ with the condition $\mathbf{r}_{l,k}\mathbf{H}^{I}_{l,k}\mathbf{w}_{l'-1} = 0$, the receive node k in cluster l constructs the receive weight vector $\mathbf{r}_{l,k}$ as follows.

$$\mathbf{r}_{l,k} = \left[\sum_{i=1}^{M-1} a_i^*\mathbf{b}_i^H\right] \Big/ \left\|\sum_{i=1}^{M-1} a_i^*\mathbf{b}_i^H\right\| \tag{6}$$

Here, the superscript $*$ indicates complex conjugate.

In addition, the transmit cluster $l-1$ knows that each receive node uses the receive weight vector to eliminate the interference. Since $|\mathbf{r}_{l,k}\mathbf{H}^{I}_{l,k}\mathbf{w}_{l'-1}| = 0$ in (4), it can be rewritten as

$$\min_{k} \log_2 \left(1 + \frac{|\mathbf{r}_{l,k}\mathbf{H}_{l,k}\mathbf{w}_{l-1}|^2}{N}\right). \tag{7}$$

To find the $\mathbf{w}_{l-1}$, the transmit cluster $l-1$ constructs $\mathbf{w}_{l-1}$ to maximize (7). However, if $\mathbf{r}_{l,k}$ is changed, the $\mathbf{w}_{l-1}$ should be modified according to $\mathbf{r}_{l,k}$. Therefore, the transmit cluster $l-1$ must simultaneously consider $\mathbf{r}_{l,k}$ and $\mathbf{w}_{l-1}$ to maximize the capacity in (7).

Toward this goal, we propose an iterative algorithm. In the algorithm, there is no need for the receive node k located in receive cluster l to feed back its receive weight vector $\mathbf{r}_{l,k}$ to update the transmit weight vector $\mathbf{w}_{l-1}$. The transmit cluster $l-1$ knows that the receive nodes will construct theirs receive weight vectors based on (6). In addition, since the transmit cluster $l-1$ has the knowledge of $\mathbf{H}^{I}_{l,k}$ and $\mathbf{w}_{l'-1}$, it is possible for the transmit cluster $l-1$ to know the receive weight vector $\mathbf{r}_{l,k}$ through (5) and (6) according to $\mathbf{w}_{l-1}$, which is updated in each iteration of the algorithm. In the proposed scheme, the transmit cluster $l-1$ constructs its transmit weight vector $\mathbf{w}_{l-1}$ using the algorithm. The receive node constructs its receive weight vector via (6) by itself.

Table 2 shows the detailed procedure for how the transmit cluster $l-1$ obtains knowledge of the receive weight vector $\mathbf{r}_{l,k}$ for all nodes in the receive cluster l, and how the transmit cluster $l-1$ constructs its transmit weight vector $\mathbf{w}_{l-1}$. In Algorithm 1 in Table 2, the parameters utilized in the algorithm are set where $n_{\max}$ is the maximum number of iterations and ε is the maximum error tolerance. In addition, the iteration index n is initialized to 1. The initial starting point of $\mathbf{r}_k(n)$ is randomly constructed as follows.

$$\mathbf{r}_k(1) = \left[\sum_{i=1}^{M} g_{k,i}\mathbf{u}_{k,i}^H\right] \Big/ \left\|\sum_{i=1}^{M} g_{k,i}\mathbf{u}_{k,i}^H\right\| \tag{8}$$

Here, $g_{k,i}$ is a zero-mean unit-variance complex Gaussian random variable and $\mathbf{u}_{k,i}^H$ is the i^{th} column vector of the unitary matrix $\mathbf{U}_k = [\mathbf{u}_{k,1}^H, \cdots, \mathbf{u}_{k,M}^H]$. Here, $\mathbf{U}_k$ is found by decomposing the channel $\mathbf{H}_{l,k} = \mathbf{U}_k\mathbf{\Sigma}_k\mathbf{V}_k^H$ via SVD where $\mathbf{\Sigma}_k$ is a $M \times K_{l-1}M$-dimensional diagonal matrix of $\mathbf{H}_{l,k}$ and $\mathbf{V}_k^H$ is a $K_{l-1}M \times K_{l-1}M$-dimensional unitary matrix.

TABLE 2. Pseudo code of the iterative algorithm for intra-network interference nulling.

Algorithm 1: Effective Intra-network Interference Nulling

Input: $\mathbf{H}_{l,k}$, $\mathbf{H}_{l,k}^{I}$, $\forall k \in \{1, \cdots, K_l\}$ and $\mathbf{w}_{l'-1}$
Output: $\mathbf{w}_{l-1}$
Set the maximum number of iterations $n_{\max}$, Convergence = **false** and the maximum error tolerance ε.
Initialize the iteration index $n = 1$.
for $k = 1$ to K_l
    $\mathbf{r}_k(n) = \left[\sum_{i}^{M} g_{k,i}\mathbf{u}_{k,i}^{H}\right] / \left\|\sum_{i}^{M} g_{k,i}\mathbf{u}_{k,i}^{H}\right\|$
end for
while Convergence = **false** and $n \le n_{\max}$ **do**
    Construct the transmit weight vector $\mathbf{w}(n)$ using GO M^2 BF.
    for $k = 1$ to K_l
        $\mathbf{r}_k(n+1) = \left[\sum_{i=1}^{M-1} a_i^*(n)\mathbf{b}_i^{H}\right] / \left\|\sum_{i=1}^{M-1} a_i^*(n)\mathbf{b}_i^{H}\right\|$
        where $\mathbf{H}_{l,k}\mathbf{w}(n) = \sum_{i=1}^{M-1} a_i(n)\mathbf{b}_i + a_M(n)\mathbf{b}_M$.
    end for
    if $\|\mathbf{r}_k(n+1) - \mathbf{r}_k(n)\| \le \varepsilon$, $\forall k \in \{1, \cdots, K_l\}$ **then**
        Convergence = **true**
    end if
    $n = n + 1$
end while
for $k = 1$ to K_l
    $\mathbf{r}_{l,k} = \mathbf{r}_k(n)$
end for
$\mathbf{w}_{l-1} = \mathbf{w}(n-1)$
return $\mathbf{w}_{l-1}$
Terminate.

Through this procedure, the transmit weight vector $\mathbf{w}(n)$ is constructed using GO M^2 BF [22] based on $\mathbf{r}_k(n)\mathbf{H}_{l,k}$, which enables $\min_k |\mathbf{r}_k(n)\mathbf{H}_{l,k}\mathbf{w}(n)|$ to be maximized. In addition, to satisfy the condition $\mathbf{r}_{l,k}\mathbf{H}_{l,k}^{I}\mathbf{w}_{l'-1} = 0$, the receive weight vector $\mathbf{r}_k(n+1)$ is updated using $a_i^*(n)$ and $\mathbf{b}_i^H$, $i \in \{1, \cdots, M-1\}$ in (6). The update procedure for $\mathbf{w}(n)$ and $\mathbf{r}_k(n)$ is repeated until $\|\mathbf{r}_k(n+1) - \mathbf{r}_k(n)\| \le \varepsilon$ for all $k \in \{1, \cdots, K_l\}$ or the iteration index n becomes greater than the maximum number of iterations $n_{\max}$. If either $\|\mathbf{r}_k(n+1) - \mathbf{r}_k(n)\| \le \varepsilon$ for all $k \in \{1, \cdots, K_l\}$ or $n > n_{\max}$ is satisfied, the algorithm determines $\mathbf{r}_{l,k}$ and $\mathbf{w}_{l-1}$ using $\mathbf{r}_k(n)$ and $\mathbf{w}(n-1)$, respectively.

Through Algorithm 1, the transmit cluster $l-1$ has knowledge of $\mathbf{r}_{l,k}$ for the receive nodes located in the receive cluster l and obtains $\mathbf{w}_{l-1}$ to maximize $\min_k |\mathbf{r}_k\mathbf{H}_{l,k}\mathbf{w}_{l-1}|$. In addition, the receive nodes construct their receive weight vectors via (6) to satisfy the condition $\mathbf{r}_{l,k}\mathbf{H}_{l,k}^{I}\mathbf{w}_{l'-1} = 0$ for intra-network interference nulling. In addition, no additional time redundancy exists when exchanging BF vectors because the transmit cluster does not need to give the information of $\mathbf{r}_{l,k}$ and $\mathbf{w}_{l-1}$ to the receive nodes. This is also true for the receive nodes. The stability of Algorithm 1 is demonstrated by proving Lemma 1.

Lemma 1: $\min_k |\mathbf{r}_k(n-1)\mathbf{H}_{l,k}\mathbf{w}(n-1)| \le \min_k |\mathbf{r}_k(n)\mathbf{H}_{l,k}\mathbf{w}(n)|$.

Proof 1: Referring to the numerical proof used in [23], here, we prove Lemma 1. In Table 2, Algorithm 1 constructs the receive weight vector $\mathbf{r}_k(n) = \left[\sum_{i=1}^{M-1} a_i^*(n-1)\mathbf{b}_i^H\right] / \left\|\sum_{i=1}^{M-1} a_i^*(n-1)\mathbf{b}_i^H\right\|$ to maximize $|\mathbf{r}_k(n)\mathbf{H}_{l,k}\mathbf{w}(n-1)|$ with the condition $\mathbf{r}_k(n)\mathbf{H}_{l,k}^{I}\mathbf{w}_{l'-1} = 0$. Therefore, since $|\mathbf{r}_k(n-1)\mathbf{H}_{l,k}\mathbf{w}(n-1)| \le |\mathbf{r}_k(n)\mathbf{H}_{l,k}\mathbf{w}(n-1)|$, $\min_k |\mathbf{r}_k(n-1)\mathbf{H}_{l,k}\mathbf{w}(n-1)| \le \min_k |\mathbf{r}_k(n)\mathbf{H}_{l,k}\mathbf{w}(n-1)|$. After the iteration index n is updated as $n+1$, the algorithm constructs $\mathbf{w}(n)$ to maximize $\min_k |\mathbf{r}_k(n)\mathbf{H}_{l,k}\mathbf{w}(n)|$. As a result, $\min_k |\mathbf{r}_k(n-1)\mathbf{H}_{l,k}\mathbf{w}(n-1)| \le \min_k |\mathbf{r}_k(n)\mathbf{H}_{l,k}\mathbf{w}(n)|$ is demonstrated.

From Lemma 1, the value of $\min_k |\mathbf{r}_k(n)\mathbf{H}_{l,k}\mathbf{w}_{l-1}(n)|$ is shown to monotonically increases with the iteration index n. This means that the value of $\min_k |\mathbf{r}_k(n)\mathbf{H}_{l,k}\mathbf{w}_{l-1}(n)|$ does not fluctuate. Therefore, it can be stated that Algorithm 1 is sufficiently stable for converging the performance of the algorithm owing to the monotonically increasing property of the algorithm. In Section V, the convergence of the algorithm is demonstrated using simulation results.

B. MULTI-HOP POWER CONTROL FOR MT

As shown in the time table in Fig. 1, to relay one symbol from the source node to the destination node, L time slots are required for the BVMS-ST when the number of clusters passed by the symbol is L. In multi-hop relay networks, the overall multi-hop capacity relies on the capacity of a link whose capacity is minimum along the link path. In addition, since only one cluster transmits the signal to the next cluster while other clusters wait their turn, intra-network interference does not occur. Therefore, the capacity of the BVMS-ST can be expressed as

$$C_{ST} = \frac{1}{L}\min_{l>2}\min_{k}\log_2\left(1 + \frac{|\mathbf{r}_{l,k}\mathbf{H}_{l,k}\mathbf{w}_{l-1}|^2}{N}\right). \quad (9)$$

In the BVMS-MT, it is assumed that two clusters are considered for concurrently transmitting the signal. Therefore, the capacity of the BVMS-MT can be written as

$$C_{MT} = \frac{2}{L}\min_{l>2}\min_{k}\log_2\left(1 + \frac{P_{l-1}|\mathbf{r}_{l,k}\mathbf{H}_{l,k}\mathbf{w}_{l-1}|^2}{P_{l'-1}|\mathbf{r}_{l,k}\mathbf{H}_{l,k}^{I}\mathbf{w}_{l'-1}|^2 + N}\right), \quad P_{l-1} + P_{l'-1} = \bar{P} \quad (10)$$

where P_{l-1} and $P_{l'-1}$ are the transmit powers of clusters $l-1$ and $l'-1$, respectively. The sum of the transmit powers is $\bar{P} = 1$ at each time. Since the transmission of each cluster becomes interference for the transmission of the other clusters in the BVMS-MT, it is necessary for each cluster to control its own transmit power to maximize the multi-hop link capacity.

To satisfy the condition $C_{MT} > C_{ST}$, both link capacities at the two clusters become greater than $\bar{C} = (L/2)C_{ST}$ as

$$\log_2\left(1 + \frac{P_{l-1}|\mathbf{r}_{l,k}\mathbf{H}_{l,k}\mathbf{w}_{l-1}|^2}{(\bar{P} - P_{l-1})|\mathbf{r}_{l,k}\mathbf{H}_{l,k}^{I}\mathbf{w}_{l'-1}|^2 + N}\right) > \bar{C}, \quad (11)$$

$$\log_2\left(1 + \frac{(\bar{P} - P_{l-1})|\mathbf{r}_{l',k}\mathbf{H}_{l',k}\mathbf{w}_{l'-1}|^2}{P_{l-1}|\mathbf{r}_{l',k}\mathbf{H}_{l',k}^{I}\mathbf{w}_{l-1}|^2 + N}\right) > \bar{C}. \quad (12)$$

Equations (11) and (12) can be rewritten in terms of P_{l-1} as

$$\frac{(2^{\bar{C}}-1)(\bar{P}|\mathbf{r}_{l,k}\mathbf{H}^I_{l,k}\mathbf{w}_{l'-1}|^2+N)}{|\mathbf{r}_{l,k}\mathbf{H}_{l,k}\mathbf{w}_{l-1}|^2+(2^{\bar{C}}-1)|\mathbf{r}_{l,k}\mathbf{H}^I_{l,k}\mathbf{w}_{l'-1}|^2}<P_{l-1}, \quad (13)$$

$$P_{l-1}<\frac{\bar{P}|\mathbf{r}_{l',k}\mathbf{H}_{l',k}\mathbf{w}_{l'-1}|^2-(2^{\bar{C}}-1)N}{(2^{\bar{C}}-1)|\mathbf{r}_{l',k}\mathbf{H}^I_{l',k}\mathbf{w}_{l-1}|^2+|\mathbf{r}_{l',k}\mathbf{H}_{l',k}\mathbf{w}_{l'-1}|^2}. \quad (14)$$

Therefore, to satisfy the condition $C_{MT} > C_{ST}$, the range of P_{l-1} can be written from (13) and (14) as

$$\alpha < P_{l-1} < \beta, \quad (15)$$

$$\alpha = \frac{(2^{\bar{C}}-1)(\bar{P}|\mathbf{r}_{l,k}\mathbf{H}^I_{l,k}\mathbf{w}_{l'-1}|^2+N)}{|\mathbf{r}_{l,k}\mathbf{H}_{l,k}\mathbf{w}_{l-1}|^2+(2^{\bar{C}}-1)|\mathbf{r}_{l,k}\mathbf{H}^I_{l,k}\mathbf{w}_{l'-1}|^2}, \quad (16)$$

$$\beta = \frac{\bar{P}|\mathbf{r}_{l',k}\mathbf{H}_{l',k}\mathbf{w}_{l'-1}|^2-(2^{\bar{C}}-1)N}{(2^{\bar{C}}-1)|\mathbf{r}_{l',k}\mathbf{H}^I_{l',k}\mathbf{w}_{l-1}|^2+|\mathbf{r}_{l',k}\mathbf{H}_{l',k}\mathbf{w}_{l'-1}|^2}. \quad (17)$$

It is possible to allocate the sub-optimal transmit power of cluster $l-1$ as $P_{l-1} = (\alpha+\beta)/2$ to satisfy the condition $C_{MT} > C_{ST}$. In addition, if each cluster employs Algorithm 1 (Table 2), $|\mathbf{r}_{l,k}\mathbf{H}^I_{l,k}\mathbf{w}_{l'-1}| = 0$ and $|\mathbf{r}_{l',k}\mathbf{H}^I_{l',k}\mathbf{w}_{l-1}| = 0$. Therefore, (15) can be rewritten as

$$\frac{(2^{\bar{C}}-1)N}{|\mathbf{r}_{l,k}\mathbf{H}_{l,k}\mathbf{w}_{l-1}|^2}<P_{l-1}<\frac{\bar{P}|\mathbf{r}_{l',k}\mathbf{H}_{l',k}\mathbf{w}_{l'-1}|^2-(2^{\bar{C}}-1)N}{|\mathbf{r}_{l',k}\mathbf{H}_{l',k}\mathbf{w}_{l'-1}|^2}. \quad (18)$$

In this case, α and β can be redefined as $\alpha = (2^{\bar{C}}-1)N/|\mathbf{r}_{l,k}\mathbf{H}_{l,k}\mathbf{w}_{l-1}|^2$ and $\beta = \{\bar{P}|\mathbf{r}_{l',k}\mathbf{H}_{l',k}\mathbf{w}_{l'-1}|^2-(2^{\bar{C}}-1)N\}/|\mathbf{r}_{l',k}\mathbf{H}_{l',k}\mathbf{w}_{l'-1}|^2$, respectively. Therefore, in EIN-VMBT, if $\alpha < \beta$, P_{l-1} for (18) is found and allocated to the cluster $l-1$ as $P_{l-1} = (\alpha+\beta)/2$. In addition, $P_{l'-1} = \bar{P} - P_{l-1}$ is allocated to the other cluster $l'-1$. In contrast, if $\alpha > \beta$, P_{l-1} does not satisfy (15) and (18) for $C_{MT} > C_{ST}$. Therefore, if the condition $\alpha < \beta$ is not satisfied by any of the clusters, ST is performed rather than MT.

C. EFFECTIVE INTER-NETWORK INTERFERENCE NULLING VMBT

Contrary to Sections IV-A and IV-B, here, it is assumed that inter-network interference is dominant to link capacity and that the influence of intra-network interference comparatively negligible. In this paper, which interference is more dominant to link capacity is determined by comparing the absolute values of inter- and intra-network interferences. The measurement process of these interferences is described in Section III. Then, the receive signal in (1) can be written as

$$\mathbf{y}_{l,k} = \mathbf{H}_{l,k}\mathbf{w}_{l-1}s + \sum_{t=1}^{T-1}\sum_{c=1}^{2}\mathbf{H}^I_{l,k,t,c}\mathbf{w}_{t,c}s_{t,c} + \mathbf{n}_{l,k}. \quad (19)$$

Under the assumption that ST is applied in each network, the receive signal in (19) can be rewritten as

$$\mathbf{y}_{l,k} = \mathbf{H}_{l,k}\mathbf{w}_{l-1}s + \sum_{t=1}^{T-1}\mathbf{H}^I_{l,k,t}\mathbf{w}_t s_t + \mathbf{n}_{l,k}, \quad (20)$$

where $\mathbf{H}^I_{l,k,t}$ is the interference channel matrix between node k in cluster l and the transmit cluster from network t, $\mathbf{w}_t$ and s_t are the transmit weight vector and network symbol, respectively. Then, the capacity of the BVMS-ST over SFN can be written as

$$C_{SFN} = \frac{W}{L}\min_{l>2}\min_{k}\log_2\left(1+\frac{|\mathbf{r}_{l,k}\mathbf{H}_{l,k}\mathbf{w}_{l-1}|^2}{\sum_{t=1}^{T-1}|\mathbf{r}_{l,k}\mathbf{H}^I_{l,k,t}\mathbf{w}_t|^2+N}\right). \quad (21)$$

In MFN, since there is no inter-network interference, the capacity of the BVMS-ST can be written as

$$C_{MFN} = \frac{W}{T}\frac{1}{L}\min_{l>2}\min_{k}\log_2\left(1+\frac{|\mathbf{r}_{l,k}\mathbf{H}_{l,k}\mathbf{w}_{l-1}|^2}{N}\right). \quad (22)$$

Let $\mathbf{b}_1, \cdots, \mathbf{b}_{M-T+1}$ be the orthonormal basis of Null$([\mathbf{H}^I_{l,k,1}\mathbf{w}_1 \cdots \mathbf{H}^I_{l,k,T-1}\mathbf{w}_{T-1}]^T)$ and let $\mathbf{b}_{M-T+2}, \cdots, \mathbf{b}_M$ be the orthonormal basis of span$([\mathbf{H}^I_{l,k,1}\mathbf{w}_1 \cdots \mathbf{H}^I_{l,k,T-1}\mathbf{w}_{T-1}]^T)$. Here, it is assumed that the number of antennas is greater than the number of networks ($T \le M$). If $T > M$, it is impossible to eliminate the inter-network interference due to lack the orthonormal basis of Null$([\mathbf{H}^I_{l,k,1}\mathbf{w}_1 \cdots \mathbf{H}^I_{l,k,T-1}\mathbf{w}_{T-1}]^T)$. Then, $\mathbf{H}_{l,k}\mathbf{w}_{l-1}$ can be written as

$$\mathbf{H}_{l,k}\mathbf{w}_{l-1} = \sum_{i=1}^{M-T+1}a_i\mathbf{b}_i + \sum_{j=M-T+2}^{M}a_j\mathbf{b}_j. \quad (23)$$

For inter-network interference nulling, the receive weight vector $\mathbf{r}_{l,k}$ must comprise $\mathbf{b}_1^H, \cdots, \mathbf{b}_{M-T+1}^H$ to satisfy the condition $\mathbf{r}_{l,k}\mathbf{H}^I_{l,k,t}\mathbf{w}_t = 0$. To maximize $|\mathbf{r}_{l,k}\mathbf{H}_{l,k}\mathbf{w}_{l-1}|$ with the condition $\mathbf{r}_{l,k}\mathbf{H}^I_{l,k,t}\mathbf{w}_t = 0$, the receive weight vector $\mathbf{r}_{l,k}$ is constructed as

$$\mathbf{r}_{l,k} = \left[\sum_{i=1}^{M-T+1}a_i^*\mathbf{b}_i^H\right] \Big/ \left\|\sum_{i=1}^{M-T+1}a_i^*\mathbf{b}_i^H\right\|. \quad (24)$$

Since $\mathbf{r}_{l,k}\mathbf{H}^I_{l,k,t}\mathbf{w}_t = 0$ via $\mathbf{r}_{l,k}$, (21) can be written as

$$\frac{W}{L}\min_{l>2}\max_{k}\log_2\left(1+\frac{|\mathbf{r}_{l,k}\mathbf{H}_{l,k}\mathbf{w}_{l-1}|^2}{N}\right). \quad (25)$$

In the case of $\mathbf{w}_{l-1}$, it is constructed using GO M^2 BF to maximize (25). However, to obtain $\mathbf{r}_{l,k}$ and $\mathbf{w}_{l-1}$, it is necessary for the transmit cluster $l-1$ to obtain knowledge of $\mathbf{H}^I_{l,k,t}$ and $\mathbf{w}_t$ via feedback of other networks, which requires additional time complexity. In addition, the signaling overhead for the transmission of the information to the transmit cluster $l-1$ is proportional to the number of networks T. Although the signaling overhead needed to obtain $\mathbf{H}^I_{l,k,t}$ and $\mathbf{w}_t$ additionally occurs, EIN-VMBT improves the overall capacity in SFNs. In addition, the information is transmitted only once to the transmit cluster $l-1$ at the initial stage before performing EIN-VMBT.

Table 3 shows the detailed procedure of the iterative algorithm for inter-network interference nulling. In Table 3,

TABLE 3. Pseudo code of the iterative algorithm for inter-network interference nulling.

Algorithm 2: Effective Inter-network Interference Nulling

Input: $\mathbf{H}_{l,k}$, $\mathbf{H}^{I}_{l,k,t}$, $\forall k \in \{1,\cdots,K_l\}$ and $\mathbf{w}_t$, $\forall t \in \{1,\cdots,T-1\}$
Output: $\mathbf{w}_{l-1}$
Set the maximum number of iterations $n_{\max}$, Convergence = **false** and the maximum error tolerance ε.
Initialize the iteration index $n = 1$.
for $k = 1$ to K_l
    $\mathbf{r}_k(n) = \left[\sum_{i}^{M} g_{k,i}\mathbf{u}_{k,i}^{H}\right] / \left\|\sum_{i}^{M} g_{k,i}\mathbf{u}_{k,i}^{H}\right\|$
end for
while Convergence = **false** and $n \leq n_{\max}$ **do**
    Construct the transmit weight vector $\mathbf{w}(n)$ using GO M^2 BF.
    for $k = 1$ to K_l
        $\mathbf{r}_k(n+1) = \left[\sum_{i=1}^{M-T+1} a_i^*(n)\mathbf{b}_i^H\right] / \left\|\sum_{i=1}^{M-T+1} a_i^*(n)\mathbf{b}_i^H\right\|$
        where $\mathbf{H}_{l,k}\mathbf{w}(n) = \sum_{i=1}^{M-T+1} a_i(n)\mathbf{b}_i + \sum_{j=M-T+2}^{M} a_j(n)\mathbf{b}_j$.
    end for
    if $\|\mathbf{r}_k(n+1) - \mathbf{r}_k(n)\| \leq \varepsilon$, $\forall k \in \{1,\cdots,K_l\}$ **then**
        Convergence = **true**
    end if
    $n = n + 1$
end while
for $k = 1$ to K_l
    $\mathbf{r}_{l,k} = \mathbf{r}_k(n)$
end for
$\mathbf{w}_{l-1} = \mathbf{w}(n-1)$
return $\mathbf{w}_{l-1}$
Terminate.

$\mathbf{r}_{l,k}$ and $\mathbf{w}_{l-1}$ can be obtained by modifying $\mathbf{r}_k(n+1) = \left[\sum_{i=1}^{M-1} a_i^*(n)\mathbf{b}_i^H\right] / \left\|\sum_{i=1}^{M-1} a_i^*(n)\mathbf{b}_i^H\right\|$ in Table 2 to $\mathbf{r}_k(n+1) = \left[\sum_{i=1}^{M-T+1} a_i^*(n)\mathbf{b}_i^H\right] / \left\|\sum_{i=1}^{M-T+1} a_i^*(n)\mathbf{b}_i^H\right\|$, where $\mathbf{H}_{l,k}\mathbf{w}(n) = \sum_{i=1}^{M-T+1} a_i(n)\mathbf{b}_i + \sum_{j=M-T+2}^{M} a_j(n)\mathbf{b}_j$. Since some of the detailed explanations of Algorithm 2 (Table 3) overlap those of Algorithm 1 (Table 2), they are omitted for brevity.

Using Algorithm 2 (Table 3), it is possible for cluster $l-1$ to obtain $\mathbf{r}_{l,k}$ and $\mathbf{w}_{l-1}$ to maximize (21). In this manner, EIN-VMBT improves the network capacity by eliminating the interference from other networks. The convergence of Algorithm 2 is demonstrated via the simulation results in Section V.

If intra- and inter-network interferences are similar in magnitude, the performance gain achieved by eliminating either type of interference is similar. Therefore, it is advantageous for each cluster to eliminate intra-network interference by utilizing Algorithm 1 rather than Algorithm 2 because Algorithm 2 requires additional channel and transmit weight vector information of other networks.

V. SIMULATION RESULTS

In this section, we evaluate the performance of the proposed EIN-VMBT through simulation by using MATLAB. As described in Section IV, since Algorithm 1 and Algorithm 2 are proposed to eliminate the intra- and inter-network interferences, respectively, two scenarios are considered in the experiments to show the effectiveness of each algorithm.

- Scenario 1: each network is the MFN. In addition, MT is performed at each network when the condition $C_{MT} > C_{ST}$ is satisfied. Thus, the dominant interference is only the intra-network interference in this scenario.
- Scenario 2: all networks use the overall frequency bandwidth (SFN). In addition, MT is not applied in this scenario. Thus, the dominant interference is only the inter-network interference in this scenario.

In each scenario, it is assumed that the distance between the two adjacent clusters is one, and that the radius of each cluster is 0.1. In addition, it is assumed that K_l nodes are distributed uniformly in each cluster. The path loss exponent η is set to 3. Under this assumption, for the verification of the proposed EIN-VMBT, we perform the simulation for the following four schemes.

- EIN-VMBT: the transmit weight vector is constructed using GO M^2 BF and the receive weight vector is constructed using Algorithm 1 (for Scenario 1) and Algorithm 2 (for Scenario 2). The multi-hop power control described in Section IV-B is applied in Scenario 1.
- IA-VMBT: the transmit weight vector is constructed using GO M^2 BF and the receive weight vector is constructed using IA.
- GO M^2 BF-Random Rx BF: the transmit weight vector is constructed using GO M^2 BF and the receive weight vector is randomly constructed.
- SVD BF: the transmit weight vector is constructed based on the first right singular vector of the channel matrix and the receive weight vector is constructed based on the left singular vector of the channel matrix.

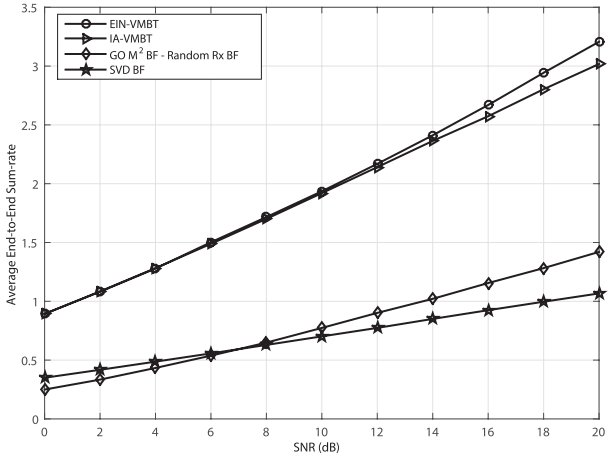

FIGURE 5. Average end-to-end sum rate for EIN-VMBT, IA-VMBT, GO M^2 BF-Random Rx BF, and SVD BF with $L = 4$, $K_l = 2$, $M = 2$, $T = 2$, and $W = 2$ in Scenario 1.

Fig. 5 shows the average end-to-end sum rate for EIN-VMBT, IA-VMBT, GO M^2 BF-Random Rx BF, and SVD BF with $L = 4$, $K_l = 2$, $M = 2$, $T = 2$, and $W = 2$ in Scenario 1. Overall, the sum rates of EIN-VMBT and IA-VMBT are greater than those of GO M^2 BF-Random

Rx BF, and SVD BF. SVD BF consumes $3(L-1)$ times to relay the signal to the destination node [22]. Therefore, the sum rate of SVD BF is worse than the other schemes due to the additional time redundancy required to relay the signal to the destination node. Its performance is even lower than that of GO M^2 BF-Random Rx BF when the SNR is greater than $8dB$ because the end-to-end sum rate relies heavily on the time latency of each protocol for multi-hop relay networking. At low SNR, the link capacity between the two clusters is important, such that the sum rate of SVD BF is greater than that of GO M^2 BF-Random Rx BF. The performance of EIN-VMBT is better than that of IA-VMBT at high SNR. As described in Section IV-A, EIN-VMBT can effectively eliminate the interference from other clusters. Therefore, the performance gain of EIN-VMBT is better than that of IA-VMBT.

Fig. 6 shows the average end-to-end sum rate for EIN-VMBT, IA-VMBT, GO M^2 BF-Random Rx BF, and SVD BF with $L = 4$, $K_l = 2$, $M = 3$, $T = 2$, and $W = 2$ in Scenario 1. Overall, the performance gain of EIN-VMBT is better than that of the other schemes. Compared with the performance shown in Fig. 5, the performance gain though the intra-network interference nulling is more evident when $M = 3$. The performance gap between EIN-VMBT and IA-VMBT increases with SNR. Thus, the interference nulling is more important than the channel gain maximization in the interference limited channel.

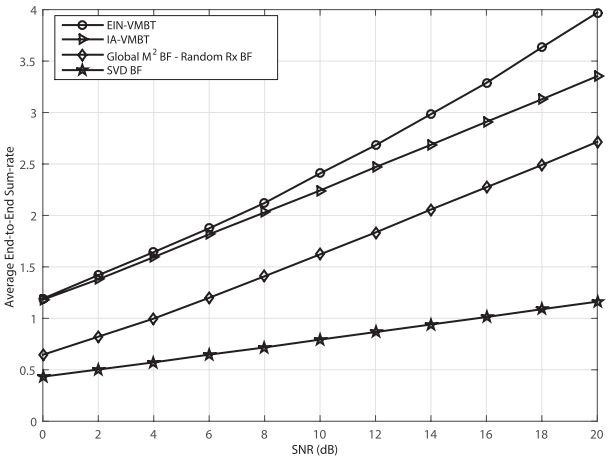

FIGURE 6. Average end-to-end sum rate for EIN-VMBT, IA-VMBT, GO M^2 BF-Random Rx BF, and SVD BF with $L = 4$, $K_l = 2$, $M = 3$, $T = 2$, and $W = 2$ in Scenario 1.

Fig. 7 shows how often ST and MT are selected in EIN-VMBT with $L = 4$, $K_l = 2$, $T = 2$, and $W = 2$ in Scenario 1. At low SNR, the number of cases in which ST is selected is greater than that of cases in which MT is selected. Contrary to low SNR, in high SNR, the number of cases in which MT is selected is greater than that of cases in which ST is selected. After all, according to definition of α and β, α is in inverse proportion to SNR and β increases with SNR. Therefore, since it is easy to satisfy the condition $\alpha < \beta$ in high SNR, it is observed that MT is more often

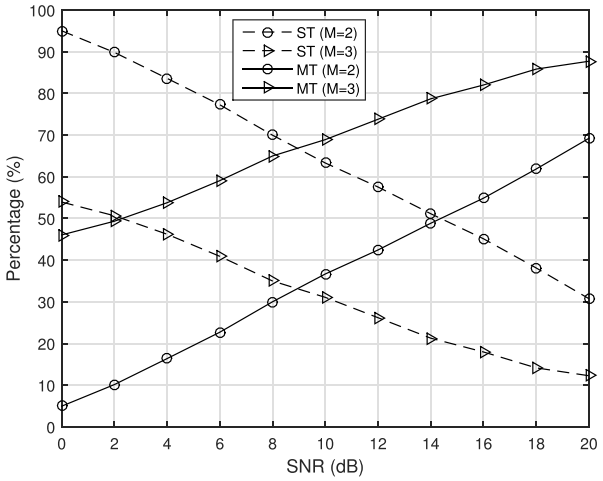

FIGURE 7. Percentage of cases in which ST and MT are selected in EIN-VMBT with $L = 4$, $K_l = 2$, $T = 2$, and $W = 2$ in Scenario 1.

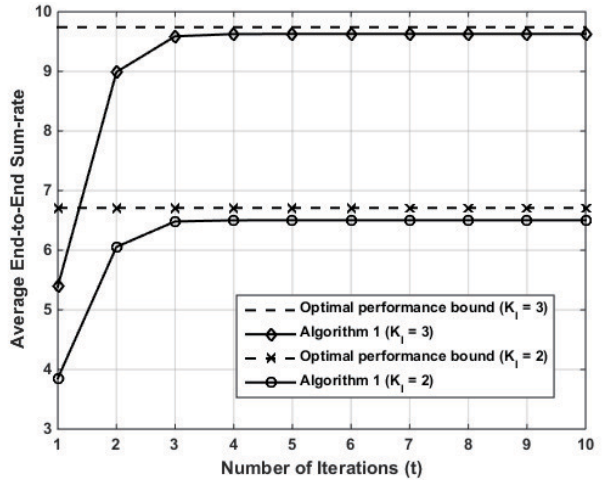

FIGURE 8. Convergence of average end-to-end sum rate according to the number of iterations for Algorithm 1 with $L = 4$ and $M = 2$ in Scenario 1.

selected in high SNR. In addition, it is also observed that the number of cases in which MT is selected with $M = 3$ is greater than that of cases in which MT is selected with $M = 2$. The diversity gain of communication channels is proportional to M. Therefore, if M increases, the condition $\alpha < \beta$ tends to be easily satisfied in even a relatively low SNR.

Fig. 8 shows the convergence of the average end-to-end sum rate according to the number of iterations for Algorithm 1 (Table 2) with $L = 4$ and $M = 2$. In Section IV-A, it is demonstrated that the value of $\min_k |\mathbf{r}_k(t)\mathbf{H}_{l,k}\mathbf{w}(t-1)|$ monotonically increases during the iteration process. The vertical axis is the average end-to-end sum rate which is calculated through the value of $\min_k |\mathbf{r}_k(t)\mathbf{H}_{l,k}\mathbf{w}(t-1)|$. To obtain the optimal performance bound of each case, the optimal weight vectors for each case are found by the brute-force search. When the number of nodes in each cluster is two and three, the average end-to-end

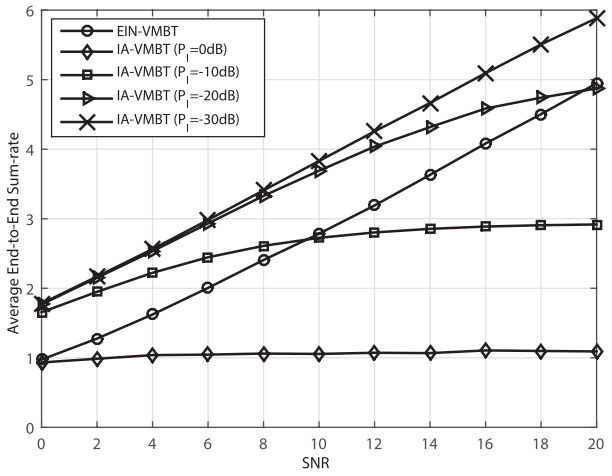

FIGURE 9. Average end-to-end sum rate for EIN-VMBT and IA-VMBT with $L = 4$, $K_I = 2$, $M = 2$, $T = 2$, and $W = 2$ in Scenario 2.

sum rate rapidly converges to a certain value a little way off the optimal performance bound after four iterations. Therefore, as shown in Fig. 8, Algorithm 1 (Table 2) has high stability.

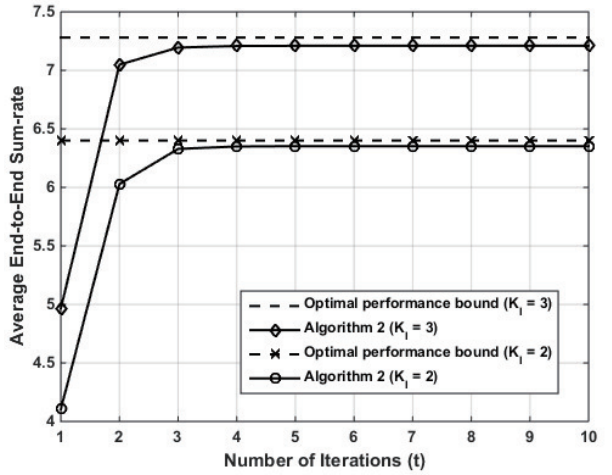

FIGURE 10. Convergence of average end-to-end sum rate according to the number of iterations for Algorithm 2 with $L = 4$, $M = 2$, $T = 2$, and $W = 2$ in Scenario 2.

Fig. 9 shows the average end-to-end sum rate for EIN-VMBT and IA-VMBT with $L = 4$, $K_I = 2$, $M = 2$, $T = 2$, and $W = 2$ in Scenario 2. The performance of IA-VMBT according to the power of interference from the other networks (P_I) is shown. As described in Section IV-C, EIN-VMBT eliminates this inter-network interference such that it demonstrates the same performance regardless of P_I. The performance of IA-VMBT becomes worse than that of EIN-VMBT when P_I is relatively high. On the other hand, when P_I is lower than $-20dB$, the performance of IA-VMBT is better than that of EIN-VMBT. Although IA-VMBT cannot eliminate inter-network interference, IA-VMBT can obtain higher performance if the interference is low enough to be ignored. On the other hand, if the interference is high, EIN-VMBT is more effective to obtain a high end-to-end sum rate.

Fig. 10 shows the convergence of Algorithm 2 (Table 3) according to the number of iterations with $L = 4$, $M = 2$, $T = 2$, and $W = 2$ in Scenario 2. In order to find the optimal performance bound of each case, the optimal weight vectors for each case are obtained by using the brute-force search. When the number of nodes in each cluster is two and three, the algorithm achieves convergence within less than five iterations. Even though the algorithm does not convenge to the optimal performance bound, the convergence points are only a little away from the optimal performance bounds. In addition, considering the convergence speed of Algorithms 1 and 2 shown in Figs. 8 and 10, EIN-VMBT is very effective for implementing a real virtual MIMO system.

VI. CONCLUSION

In general, conventional BVMS- and VMBT-based schemes have been developed in a limited environment under the assumption that only one cluster transmits signals to the next cluster to avoid intra-network interference. In addition, to avoid inter-network interference, each network is assumed to be an MFN. Therefore, it is difficult to apply these schemes to a real system. In addition, in a practical environment, there is a case wherein using MT or the same frequency band is better for achieving improved performance. To alleviate this limitation and achieve high end-to-end sum rate over intra- and inter-network interferences' environments, a new effective interference nulling technique called EIN is proposed to VMBT for MT over SFN. In EIN-VMBT, the intra- and inter-network interferences are effectively eliminated. In addition, no additional time redundancy related to BF vector information exchange among the transmit cluster and receive nodes exist. Through simulation results, it is verified that a high average end-to-end sum rate can be achieved when the proposed EIN-VMBT is applied. In addition, the convergence of the proposed scheme is achieved within less than five iterations on average. Therefore, it may be applicable for real virtual MIMO systems.

REFERENCES

[1] J. Wu, K. Ota, M. Dong, and C. Li, "A hierarchical security framework for defending against sophisticated attacks on wireless sensor networks in smart cities," *IEEE Access*, vol. 4, pp. 416–424, Jan. 2016.

[2] E. Fadel *et al.*, "A survey on wireless sensor networks for smart grid," *Comput. Commun.*, vol. 71, no. 1, pp. 22–33, Nov. 2015.

[3] J. Zhu, Y. Song, D. Jiang, and H. Song, "Multi-armed bandit channel access scheme with cognitive radio technology in wireless sensor networks for the Internet of Things," *IEEE Access*, vol. 4, pp. 4609–4617, Aug. 2016.

[4] D. G. Reina *et al.*, "A survey on multihop ad hoc networks for disaster response scenarios," *Int. J. Distrib. Sensor Netw.*, vol. 11, no. 10, p. 647037, Jan. 2015.

[5] S. Misra, M. Reisslein, and G. Xue, "A survey of multimedia streaming in wireless sensor networks," *IEEE Commun. Surveys Tuts.*, vol. 10, no. 4, pp. 18–39, 4th Quart., 2008.

[6] I. F. Akyildiz, T. Melodia, and K. R. Chowdhury, "Wireless multimedia sensor networks: Applications and testbeds," *Proc. IEEE*, vol. 96, no. 10, pp. 1588–1605, Oct. 2008.

[7] A. Papadogiannis, E. Hardouin, and D. Gesbert, "Decentralising multicell cooperative processing: A novel robust framework," *EURASIP J. Wireless Commun. Netw.*, vol. 2009, no. 1, p. 890685, Dec. 2009, doi: 10.1155/2009/890685.
[8] S. Han, Q. Zhang, and C. Yang, "Distributed coordinated multi-point downlink transmission with over-the-air communication," in *Proc. IEEE 5th Int. ICST Conf. Commun. Netw. China (CHINACOM)*, Beijing, China, Aug. 2010, pp. 1–5.
[9] R. Zhang and L. Hanzo, "Joint and distributed linear precoding for centralised and decentralised multicell processing," in *Proc. IEEE 72nd Veh. Technol. Conf. Fall (VTC-Fall)*, Ottawa, ON, Canada, Sep. 2010, pp. 1–5.
[10] N. Seifi, R. W. Heath, Jr., M. Coldrey, and T. Svensson, "Adaptive multicell 3-D beamforming in multiantenna cellular networks," *IEEE Trans. Veh. Technol.*, vol. 65, no. 8, pp. 6217–6231, Aug. 2016.
[11] H. Son, J. Park, and S. Lee, "Hierarchical modulation-based cooperation utilizing relay-assistant full-duplex diversity," *Wireless Netw.*, vol. 17, no. 3, pp. 583–595, Apr. 2011.
[12] J. Park, H. Son, and S. Lee, "Throughput and QoS improvement via fixed relay station cooperated beam-forming," *IEEE Trans. Wireless Commun.*, vol. 8, no. 5, pp. 2400–2409, May 2009.
[13] J. Park and S. Lee, "MIMO beamforming for QoS enhancement via analog, digital and hybrid relaying," *IEEE Trans. Broadcast.*, vol. 56, no. 4, pp. 494–503, Dec. 2010.
[14] Y. Yuan, Z. He, and M. Chen, "Virtual MIMO-based cross-layer design for wireless sensor networks," *IEEE Trans. Veh. Technol.*, vol. 55, no. 3, pp. 856–864, May 2006.
[15] S. K. Jayaweera, "Virtual MIMO-based cooperative communication for energy-constrained wireless sensor networks," *IEEE Trans. Wireless Commun.*, vol. 5, no. 5, pp. 984–989, May 2006.
[16] Y. Rong and Y. Hua, "Optimal power schedule for distributed MIMO links," *IEEE Trans. Wireless Commun.*, vol. 7, no. 8, pp. 2896–2900, Aug. 2008.
[17] B. Chen and M. J. Gans, "MIMO communications in ad hoc networks," *IEEE Trans. Signal Process.*, vol. 54, no. 7, pp. 2773–2783, Jul. 2006.
[18] C. Liang and K. R. Dandekar, "Power management in MIMO ad hoc networks: A game-theoretic approach," *IEEE Trans. Wireless Commun.*, vol. 6, no. 4, pp. 1164–1170, Apr. 2007.
[19] H. Huang, H. Barani, and H. Al-Azzawi. (2014). "Network multiple-input and multiple-output for wireless local area networks." [Online]. Available: https://arxiv.org/abs/1402.1882
[20] H. V. Balan, R. Rogalin, A. Michaloliakos, K. Psounis, and G. Caire, "AirSync: Enabling distributed multiuser MIMO with full spatial multiplexing," *IEEE/ACM Trans. Netw.*, vol. 21, no. 6, pp. 1681–1695, Dec. 2013.
[21] X. Zhang, K. Sundaresan, M. A. A. Khojastepour, S. Rangarajan, and K. G. Shin, "NEMOx: Scalable network MIMO for wireless networks," in *Proc. 19th Annu. Int. Conf. Mobile Comput. Netw.*, Miami, FL, USA, Sep. 2013, pp. 453–464.
[22] J. Park and S. Lee, "M^2-m^2 beamforming for virtual MIMO broadcasting in multi-hop relay networks," *IEEE J. Sel. Areas Commun.*, vol. 30, no. 8, pp. 1358–1369, Sep. 2012.
[23] B. Kwon, J. Park, and S. Lee, "Virtual MIMO broadcasting transceiver design for multi-hop relay networks," *Digit. Signal Process.*, vol. 46, pp. 97–107, Nov. 2015.
[24] Q. H. Spencer, A. L. Swindlehurst, and M. Haardt, "Zero-forcing methods for downlink spatial multiplexing in multiuser MIMO channels," *IEEE Trans. Signal Process.*, vol. 52, no. 2, pp. 461–471, Feb. 2004.
[25] T. Yoo and A. Goldsmith, "On the optimality of multiantenna broadcast scheduling using zero-forcing beamforming," *IEEE J. Sel. Areas Commun.*, vol. 24, no. 3, pp. 528–541, Mar. 2006.
[26] P. S. Udupa and J. S. Lehnert, "Optimizing zero-forcing precoders for MIMO broadcast systems," *IEEE Trans. Commun.*, vol. 55, no. 8, pp. 1516–1524, Aug. 2007.
[27] Y.-C. Tseng, C.-S. Hsu, and T.-Y. Hsieh, "Power-saving protocols for IEEE 802.11-based multi-hop ad hoc networks," *Comput. Netw.*, vol. 43, no. 3, pp. 317–337, Oct. 2003.
[28] W. Ye, J. Heidemann, and D. Estrin, "Medium access control with coordinated adaptive sleeping for wireless sensor networks," *IEEE/ACM Trans. Netw.*, vol. 12, no. 3, pp. 493–506, Jun. 2004.

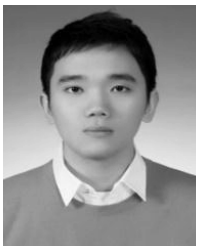

BEOM KWON was born in South Korea in 1989. He received the B.S. degree in electrical and electronic engineering from Soongsil University, Seoul, South Korea, in 2012. He is currently pursuing the M.S. and Ph.D. degrees with the Multidimensional Insight Laboratory, Yonsei University. His research interests are in the area of wireless communication networks, computer vision, and machine learning.

SANGHOON LEE (M'05–SM'12) received the B.S. degree from Yonsei University, Seoul, South Korea, in 1989, the M.S. degree from the Korea Advanced Institute of Science and Technology in 1991, and the Ph.D. degree from The University of Texas at Austin in 2000, all in E.E. From 1991 to 1996, he was with Korea Telecom. From 1999 to 2002, he was with Lucent Technologies on 3G wireless and multimedia networks. In 2003, he joined the Faculty of the Department of Electrical and Electronics Engineering, Yonsei University, where he is currently a Full Professor. His research interests include image/video quality assessment, computer vision, graphics, cloud computing, and multimedia communications and wireless networks. He has been serving as a member of the Technical Committee of the IEEE Multimedia Signal Processing since 2016, the IEEE IVMSP Technical Committee since 2014, and the APSIPA IVM TC Vice Chair 2016. He received the 2015 Yonsei Academic Award from Yonsei University, the 2012 Special Service Award from the IEEE Broadcast Technology Society, and the 2013 Special Service Award from the IEEE Signal Processing Society. He was the Technical Program Co-Chair of the International Conference on Information Networking in 2014, and the Global 3-D Forum in 2012 and in 2013, and the General Chair of the 2013 IEEE IVMSP Workshop. He also served as a special issue Guest Editor of the IEEE Transactions on Image Processing in 2013, and an Editor of the *Journal of Communications and Networks* from 2009 to 2015. He was an Associate Editor of the IEEE Transactions on Image Processing from 2010 to 2014. He has been an Associate Editor of IEEE Signal Processing Letters since 2014, and the *Journal of Electronic Imaging* since 2015, and the Chair of the IEEE P3333.1 Quality Assessment Working Group since 2011.